

# High frequency dynamics in a monatomic glass.

T. Scopigno<sup>1</sup>, R. Di Leonardo<sup>1</sup>, G. Ruocco<sup>1</sup>

<sup>1</sup>*Dipartimento di Fisica and INFM, Università di Roma "La Sapienza", I-00185, Roma, Italy.*

A.Q.R. Baron<sup>2</sup>, S. Tsutsui<sup>2</sup>

<sup>2</sup>*SPring-8/JASRI, 1-1-1 Kouto, Mikazuki-cho, Sayo-gun, Hyogo-ken 679-5198 Japan.*

F. Bossard<sup>3</sup> S.N.Yannopoulos<sup>3</sup>

<sup>3</sup>*Foundation for Research and Technology - Hellas,  
Institute of Chemical Engineering and High-Temperature Chemical Processes,  
FORTH-ICE/HT, P.O. Box 1414, GR-265 00 Patras, Greece.*

(Dated: June 16, 2018)

The high frequency dynamics of glassy Selenium has been studied by Inelastic X-ray Scattering at beamline BL35XU (SPring-8). The high quality of the data allows one to pinpoint the existence of a dispersing acoustic mode for wavevectors ( $Q$ ) of  $1.5 < Q < 12.5 \text{ nm}^{-1}$ , helping to clarify a previous contradiction between experimental and numerical results. The sound velocity shows a positive dispersion, exceeding the hydrodynamic value by  $\approx 10\%$  at  $Q < 3.5 \text{ nm}^{-1}$ . The  $Q^2$  dependence of the sound attenuation  $\Gamma(Q)$ , reported for other glasses, is found to be the low- $Q$  limit of a more general  $\Gamma(Q) \propto \Omega(Q)^2$  law which applies also to the higher  $Q$  region, where  $\Omega(Q) \propto Q$  no longer holds.

PACS numbers: 61.43.Fs; 63.50.+x; 61.10.Eq

The possibility of high frequency sound propagation in disordered systems has stimulated a large number of investigations in the last twenty years [1]. In particular, in glassy systems, the existence of short wavelength acoustic modes can be traced back to the pioneering numerical simulation works of Grest, Nagel and Rahman [2]. The details of these high frequency excitations are closely interwoven with some well known "anomalies" such as the excess of vibrational density of state (the so-called Boson Peak) or the thermal conductivity plateau observed in the  $1 < T < 10 \text{ K}$  region, which mark non-trivial distinctions from the crystalline state [3]. In this respect, glassy selenium constitutes a system of paramount importance. Not only does it exhibit all the above mentioned anomalies [3, 4], but it is also interesting for its technological impact due to the well known high sensitiveness to photo-induced effects [5].

Crystalline selenium exists at least in three different atomic arrangements. The more stable is the hexagonal form in which the atoms are distributed along parallel chains with the threefold spiral along the  $c$  axis. The monoclinic phases (a and b) are metastable and are both characterized by eight-membered  $\text{Se}_8$ -rings. Rhombohedral and cubic Se have also been reported. As the energy difference between the two main crystal phases - hexagonal and monoclinic - is very small compared to  $k_B T_g$  ( $T_g=303 \text{ K}$  being the glass transition temperature), the competition between the two local structures endows to selenium an excellent glass-forming ability; an extremely rare feature for a monatomic system. For the above reasons, glassy selenium (g-Se) has been widely investigated in the past by a large variety of experimental techniques, and also several numerical investigations have

been reported [6, 7, 8, 9, 10]. This notwithstanding, some crucial aspects related to the features of the microscopic collective dynamics at wavelength comprising few atomic units are still unknown. More specifically, numerical investigations report in this momentum transfer  $Q$  region evidence of collective modes up to frequencies as high as  $8 - 10 \text{ meV}$ , characterized by a well defined phonon-like dispersion curve [8]. However, based on recent inelastic neutron scattering (INS) experiments, a localization threshold of  $3 - 4 \text{ meV}$  ( $Q \approx 3 \text{ nm}^{-1}$ ) was proposed, above which the longitudinal acoustic dynamics became strongly overdamped [10].

In this letter we present the first direct determination of the coherent dynamic structure factor by means of Inelastic X-ray Scattering (IXS) in g-Se. The extremely favorable inelastic/elastic intensity ratio allows for a reliable analysis of the collective dynamics. We find evidence for an acoustic-like propagating mode with a sound velocity exceeding the hydrodynamic value, a signature of a relaxation process active over the probed timescale. A quadratic dependence of the sound attenuation on the mode frequency is observed all over the explored region, generalizing the  $Q^2$  law observed at small  $Q$  in other glasses.

The experiment was performed at the high resolution inelastic scattering beamline (BL35XU) [11] of SPring-8 in Hyogo prefecture, Japan. High resolution was obtained using the (11 11 11) reflection of perfect silicon crystals while a backscattering geometry ( $\frac{\pi}{2} - \theta_B \approx 0.3 \text{ mrad}$ ) was used (for both monochromator and analyzers) in order to obtain large angular acceptance. A grazing incidence geometry for the backscattering monochromator was crucial to avoid heat-load broadening of the resolu-

tion due to the x-ray power load. The flux onto the sample was  $\approx 3 \times 10^9$  photons/sec (100 mA electron beam current) in a 0.8 meV bandwidth at 21.747 keV and a spot size of 80  $\mu\text{m}$  diameter FWHM (full width at half maximum). The use of 4 analyzer crystals, placed with 0.78 degree spacing on the 10 m two-theta arm (horizontal scattering plane), and 4 independent detectors, allowed collection of 4 momentum transfers simultaneously. Slits in front of the analyzer crystals limited their acceptance to  $0.24 \text{ nm}^{-1}$  in the scattering plane. The over-all resolution of the spectrometer was then 1.5 to 1.8 meV, depending on the analyzer crystal. Typical data collection times were 200 s/bin, where the bin size was fixed at 0.25 meV.

Elemental Selenium (purity 99.999 %) was purchased from Cerac Inc. The 3 mm Se shots were placed on a temperature controlled flat surface which was heated to few degrees above the melting point of the crystal ( $T_m = 494 \text{ K}$ ). Final thick-film samples were obtained by applying to the viscous melt a mechanical press and fast cooling far below the glass transition temperature. The thickness of the Se specimens controlled by the pressure strength, lies between 50-100  $\mu\text{m}$ , which is very close to the optimum for matching the absorption length of the X-rays ( $\mu^{-1} = 50 \mu\text{m}$ ). The obtained flakes were allowed to anneal near  $T_g$  and the IXS experiment was performed at  $T = 295 \text{ K}$ .

In Fig.1 we report the measured spectra at selected values of (fixed) momentum transfer. Clear evidence of an inelastic mode, at the wings of the elastic peak, can be observed. The behavior of the energy shift of this mode vs. the momentum transfer strongly resembles a phonon-like propagating mode. The high inelastic/elastic ratio allows for a detailed analysis of this mode less ambiguously than in previously studied glasses [12, 13, 14, 15, 16, 17, 18]. Following the prescription of generalized hydrodynamics [19], and modeling the vibrational dynamics as a Markovian process with an instantaneous second order memory function, one ends up with a damped harmonic oscillator line shape to represent the dynamic structure factor  $S(Q, \omega)$ :

$$\frac{S(Q, \omega)}{S(Q)} = \left[ f(Q)\delta(\omega) + \frac{1 - f(Q)}{\pi} \frac{\Omega^2(Q)\Gamma(Q)}{(\omega^2 - \Omega^2(Q))^2 + \omega^2\Gamma^2(Q)} \right] \quad (1)$$

The parameters  $\Omega(Q)$  and  $\Gamma(Q)$  represent the characteristic frequency and attenuation of the mode,  $S(Q)$  is the static structure factor, while  $f(Q)$ , the non-ergodicity factor, is related to the inelastic/elastic ratio.

The measured intensity is proportional to the convolution between the instrumental resolution  $R(\omega)$  and the dynamic structure factor modified to account for the detailed balance condition, namely:

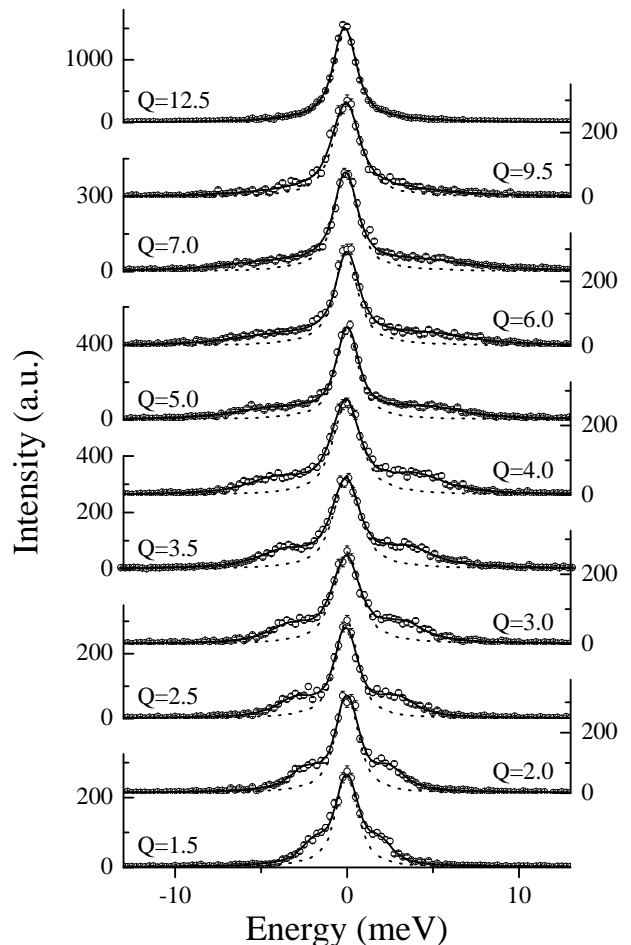


FIG. 1: IXS spectra of glassy selenium (open dots) measured for several momentum transfers, as indicated by the labels ( $\text{nm}^{-1}$ ). Also reported are the instrument resolution (dotted line) and the best fit lineshape according to the model discussed in the text (full line).

$$I(Q, \omega) = e(Q) \int d\omega' \frac{\hbar\omega'/KT}{1 - e^{-\hbar\omega'/KT}} S(Q, \omega') R(\omega - \omega') \quad (2)$$

with  $e(Q)$  being a factor accounting for the efficiency of the analyzers, sample thickness, the atomic form factors and other angular-dependent instrumental correction factors [25]. The best fitted lineshapes, obtained with Eq. 2 are reported in Fig. 1 (full lines). It is evident that our model function, representing a single excitation model, satisfactorily accounts for the measured response.

The results of the present IXS experiment are summarized in Fig. 2, where we report the  $Q$ -dependence of the three shape parameters together with that of the apparent sound velocity  $c(Q) = \Omega(Q)/Q$ . Figure 2a) presents compelling evidence for the existence of an acoustic-like longitudinal branch, which is well defined up to the higher investigated momentum transfer ( $Q = 12.5 \text{ nm}^{-1}$ ).

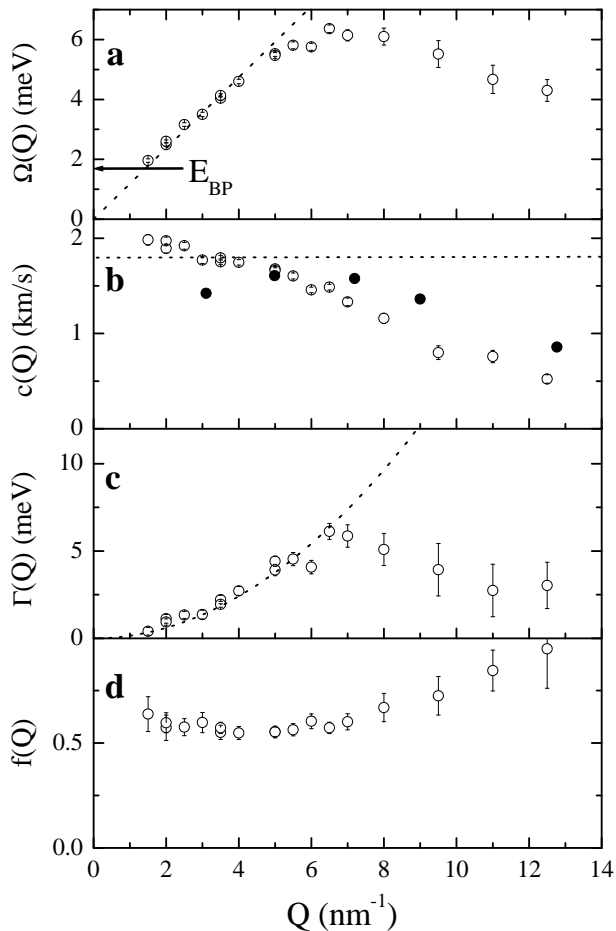


FIG. 2: Relevant parameters obtained by fitting the IXS measurements. (a) Maximum of the longitudinal current correlation function (open dots) and the hydrodynamic dispersion [6] (dotted line). (b) Apparent sound velocity,  $\Omega(Q)/Q$  (open dots), molecular dynamics results [8] (full dots), and the hydrodynamic value (dotted line). (c) Sound attenuation (open dots) with the best  $Q^2$  fit:  $\Gamma = 0.15Q^2$  with  $\Gamma$  and  $Q$  expressed in meV and  $\text{nm}^{-1}$ , respectively (dotted line). (d) Non-ergodicity parameter as obtained from the inelastic/elastic ratio

No evidence of localization is found at  $Q=3 \text{ nm}^{-1}$  as it has been suggested in Ref.[10]. Moreover, the dispersion curve extends well beyond the boson peak frequency ( $E_{BP} \approx 1.7 \text{ meV}$  in g-Se at  $T = 300 \text{ K}$  [6]), confirming earlier observations reported in other glasses [20].

The data from the INS experiment [10] have been analyzed assuming the simultaneous presence, in the same  $Q$  region under investigation here, of a longitudinal acoustic (LA) mode and a local optic-like mode. The model that was utilized to describe the LA mode implied the presence of a crossover between a propagating and localized regime, and this crossover was found to be located around  $Q \approx 3 \text{ nm}^{-1}$  [10]. In contrast, MD simulations have shown the existence of a well defined dis-

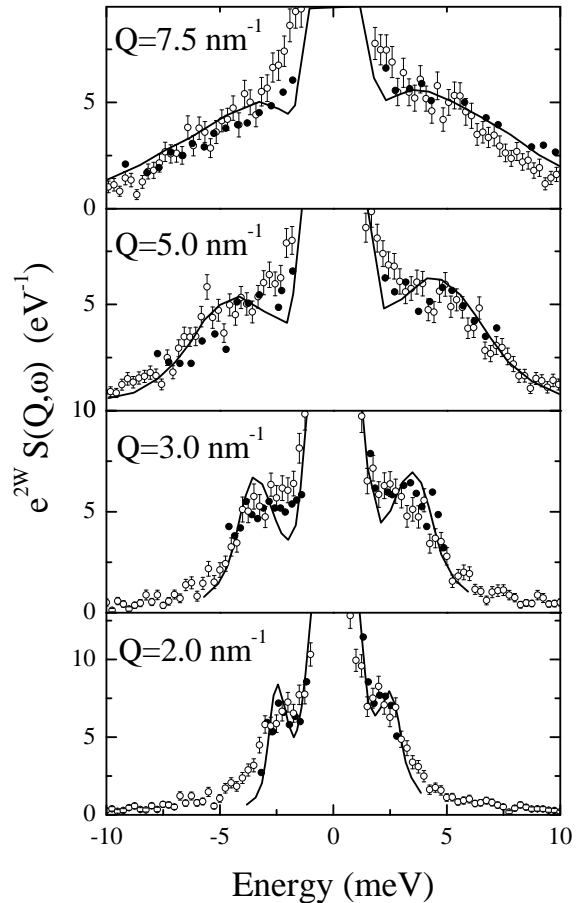


FIG. 3: Comparison between the IXS results (open dots and error bar) and previous INS measurements from Ref. [10]. Also reported is the best fit to the INS data (full line)

persion curve up to the edge of the first pseudo-Brillouin zone ( $Q \approx 10 \text{ nm}^{-1}$ ). This is shown in Fig.2b, where the sound velocity,  $c(Q)$ , derived by MD (full dots) and by the present work (open dots) are reported. In Fig. 3, we plot the data from the INS experiment [10] (full dots) alongside with our IXS data (open dots) with the latter scaled to optimize the overlap in the common frequency range. As can be observed, the two sets of data are in reasonable agreement. The small differences at the base of the elastic peak are expected given the difference in INS and IXS resolution functions: while both have  $\approx 1.5 \text{ meV}$  FWHM, the IXS resolution is approximately Lorentzian, while the INS resolution is Gaussian. The INS measurements, even pushing the limit of the technique at its maximum, span only a limited range in energy due to kinematic restrictions. This leads to best-fit lineshapes which exaggerate the 'humps' between zero to five meV (full line in Fig. 3) and ultimately do not reproduce the IXS spectra, measured over a much wider energy region ( $-25 < E < 25 \text{ meV}$ ).

The extrapolated limit of the apparent sound velocity  $\lim_{Q \rightarrow 0} c(Q) \approx 2000$  m/s (Fig. 2b), as measured by IXS, falls above the hydrodynamic value ( $c_0 = 1800$  m/s), suggesting the presence of a possible mild positive dispersion effect. As recently reported for another system [21], this effect may be due to a residual relaxation process -active in the glass- and with relaxation time in the ps range. The origin of this process is not clear at present, it could tentatively be associated with the presence of topological disorder which modifies the hydrodynamic sound properties at wavelength comparable with the mean interparticle distances [22].

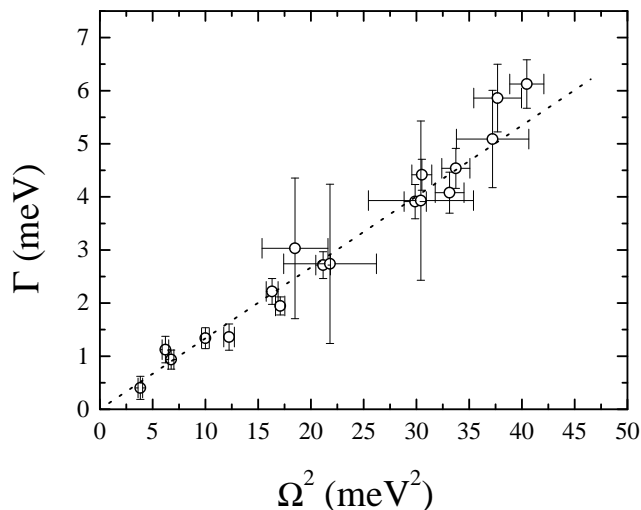


FIG. 4: Sound damping vs. square of the excitation frequency. The quadratic dependence on the wavevector  $Q^2$  shown in Fig. 2c turns out to be the low  $Q$  limit of the more general dependence shown here.

The sound attenuation parameter  $\Gamma(Q)$  (Fig. 2c) is found to be compatible with a  $Q^2$  law, up to  $Q$ 's value where the dispersion relation is linear (i. e.  $c(Q) \approx \text{constant}$ ) ( $Q < 5\text{nm}^{-1}$ ). This coincidence suggests a *common* breakdown of the linear and quadratic laws for  $\Omega(Q)$  and  $\Gamma(Q)$  respectively which is expected to be caused by structural effects, i.e. by the  $Q$ -dependence of the static structure factor [19]. In order to remove this structural dependence we report in Fig. 4 the value of sound attenuation parameter plotted against the excitation frequency for all measured  $Q$  values. As can be observed a simple power law relation now extends up to the whole explored momentum region. The best fitted law turns out to be  $\Gamma \propto \Omega^\alpha$  with  $\alpha=2.15 \pm 0.10$ . The present observation spotlights another aspect which needs to be encompassed in the explanation of the ubiquitous [12, 13, 14, 15, 16]  $Q^2$  (or  $\Omega(Q)^2$ ) dependence which is not yet fully explained.

Finally we emphasize how the combination of IXS technique and generalized hydrodynamics provides a powerful tool to extract information about the non-ergodicity

factor  $f(Q)$ , i. e. the long time plateau of the intermediate scattering function once the structural arrest is attained. This quantity is reported Fig. 2d. It should be stressed that  $f(Q)$  is a true "shape" parameter (i. e. it does not depend on the absolute intensity, a quantity more difficult to access experimentally) and, in particular, it is related to the elastic-to-inelastic intensity ratio. g-Se is found to have a remarkably low  $f(Q)$  value when compared to other glasses at  $T_g$ , a feature which allow a reliable lineshape analysis due to the extremely favorable inelastic/elastic signal. This low  $f(Q)$  value of selenium mirrors the high fragility, according to the Angell classification scheme [23], in agreement with recent findings that link the value of the fragility with that of  $f(Q \rightarrow 0)$  at  $T_g$  [24].

In conclusion, we presented an accurate measurement of the dynamic structure factor in g-Se, taking advantage of the state of the art capabilities of a new IXS facility. The inelastic/elastic signal is particularly favorable in this system. Therefore, exploiting the lack of kinematic constrains and the very good statistics, we have been able to perform a robust lineshape analysis in an extended and previously unexplored momentum-energy region. We found evidence for a well defined longitudinal acoustic mode extending all the way beyond the first pseudo-Brillouin zone, characterized by dispersion and attenuation properties typical of other glass forming materials. In particular, the boson peak frequency lies in the linear dispersion region, thus suggesting a link between this universal feature of glasses and the reported high frequency acoustic excitation. Moreover, the presence of such a well defined mode allows to get new insight into the high frequency sound attenuation issue. Specifically, a quadratic dependence of the sound attenuation on the mode frequency extends the  $Q^2$  law holding in a smaller range and observed in other glass formers. Such an observation indicates the prominent role of the excitation frequency rather than of its wavevector, and certainly calls for further investigations.

The synchrotron radiation experiment was performed at the SPring-8 with the approval of the Japan Synchrotron Radiation Research Institute (JASRI) (Proposal No. 2003A0357-ND3-279).

- 
- [1] K. Ngai, ed., *Proc. of the 4th International Discussion Meeting on Relaxations in Complex Systems*, vol. 307-310 (2002), special Issues of the Journal of Non-Crystalline Solids.
  - [2] G. S. Grest, S. R. Nagel, and A. Rahman, *Phys. Rev. Lett.* **49**, 1271 (1982).
  - [3] R. Pohl, X. Liu, and E. J. Thompson, *Rev. Mod. Phys.* **74**, 991 (2002).
  - [4] U. Buchenau, Y. M. Galperin, V. L. Gurevich, D. A. Parshin, M. A. Ramos, and H. R. Schober, *Phys. Rev. B*

- 46**, 2798 (1992).
- [5] Kolobov, ed., *Photo-induced Metastability in Amorphous Semiconductors* (Wiley-VCH, Berlin, 2003).
- [6] P. Andonov, *J. Non-Cryst. Solids* **47**, 297 (1982).
- [7] W. A. Phillips, U. Buchenau, N. Nucker, A. J. Dianoux, and W. Petry, *Phys. Rev. Lett.* **63**, 2381 (1989).
- [8] M. Garcia-Hernandez, F. J. Bermejo, B. Fak, J. L. Martinez, E. Enciso, N. G. Almarza, and A. Criado, *Phys. Rev. B* **48**, 149 (1993).
- [9] D. Caprion and H. R. Schober, *Phys. Rev. B* **62**, 3709 (2000).
- [10] M. Foret, B. Hehlen, G. Taillades, E. Courtens, R. Vacher, H. Casalta, and B. Dorner, *Phys. Rev. Lett.* **81**, 2100 (1998).
- [11] A. Q. R. Baron, Y. Tanaka, S. Goto, K. Takeshita, T. Matsushita, and T. Ishikawa, *J. Phys. Chem. Solids* **61**, 461 (2000).
- [12] P. Benassi, M. Krisch, C. Masciovecchio, V. Mazzacurati, G. Monaco, G. Ruocco, F. Sette, and R. Verbeni, *Phys. Rev. Lett.* **77**, 3835 (1996).
- [13] C. Masciovecchio, G. Ruocco, F. Sette, M. Krisch, R. Verbeni, U. Bergmann, and M. Soltwisch, *Phys. Rev. Lett.* **76**, 3356 (1996).
- [14] O. Pilla, A. Cunsolo, A. Fontana, C. Masciovecchio, G. Monaco, M. Montagna, G. Ruocco, T. Scopigno, and F. Sette, *Phys. Rev. Lett.* **85**, 2136 (2000).
- [15] A. Matic, L. Börjesson, G. Ruocco, C. Masciovecchio, A. Mermet, F. Sette, and R. Verbeni, *Europhys. Lett.* **54**, 77 (2001).
- [16] A. Matic, D. Engberg, C. Masciovecchio, and L. Borjesson, *Phys. Rev. Lett.* **86**, 3803 (2001).
- [17] M. Foret, E. Courtens, R. Vacher, and J.-B. Suck, *Phys. Rev. Lett.* **77**, 3831 (1996).
- [18] B. Rufflé, M. Foret, E. Courtens, R. Vacher, and G. Monaco, *Phys. Rev. Lett.* **90**, 095502 (2003).
- [19] J. P. Boon and S. Yip, *Molecular Hydrodynamics* (McGraw-Hill, NewYork, 1980).
- [20] F. Sette, M. Krisch, C. Masciovecchio, G. Ruocco, and G. Monaco, *Science* **280**, 1550 (1998).
- [21] B. Ruzicka, T. Scopigno, S. Caponi, A. Fontana, P. Giura, G. Monaco, O. Pilla, E. Pontecorvo, G. Ruocco, and F. Sette (Submitted to *Phys. Rev. Lett.*).
- [22] G. Ruocco, F. Sette, R. Di Leonardo, G. Monaco, M. Sampoli, T. Scopigno, and G. Vilianni, *Phys. Rev. Lett.* **84**, 5788 (2000).
- [23] C. A. Angell, *Science* **267**, 1924 (1995).
- [24] T. Scopigno, G. Ruocco, F. Sette, and G. Monaco, *Science* **302**, 849 (2003).
- [25]  $e(Q)$  does not introduce a new fitting parameters, but prevents the determination of  $S(Q)$  from the scattered intensity